Plant, Cell and Environment (2007) **30**, 892–909 doi: 10.1111/j.1365-3040.2007.01676.x

Modelling advection and diffusion of water isotopologues in leaves

MATTHIAS CUNTZ[1]*, JÉRÔME OGÉE[2], GRAHAM D. FARQUHAR[1], PHILIPPE PEYLIN[3] & LUCAS A. CERNUSAK[1†]

[1]*Environmental Biology Group, Research School of Biological Sciences, Australian National University, Canberra, Australia,* [2]*Functional Ecology and Environmental Physics (EPHYSE), INRA, Villenave d'Ornon, France and* [3]*BiOEMCO, CNRS/INRA/UPMC, Grignon, France*

ABSTRACT

We described advection and diffusion of water isotopologues in leaves in the non-steady state, applied specifically to amphistomatous leaves. This explains the isotopic enrichment of leaf water from the xylem to the mesophyll, and we showed how it relates to earlier models of leaf water enrichment in non-steady state. The effective length or tortuosity factor of isotopologue movement in leaves is unknown and, therefore, is a fitted parameter in the model. We compared the advection–diffusion model to previously published data sets for *Lupinus angustifolius* and *Eucalyptus globulus*. Night-time stomatal conductance was not measured in either data set and is therefore another fitted parameter. The model compared very well with the observations of bulk mesophyll water during the whole diel cycle. It compared well with the enrichment at the evaporative sites during the day but showed some deviations at night for *E. globulus*. It became clear from our analysis that night-time stomatal conductance should be measured in the future and that the temperature dependence of the tracer diffusivities should be accounted for. However, varying mesophyll water volume did not seem critical for obtaining a good prediction of leaf water enrichment, at least in our data sets. In addition, observations of single diurnal cycles do not seem to constrain the effective length that relates to the tortuosity of the water path in the mesophyll. Finally, we showed when simpler models of leaf water enrichment were suitable for applications of leaf water isotopes once weighted with the appropriate gas exchange flux. We showed that taking an unsuitable leaf water enrichment model could lead to large biases when cumulated over only 1 day.

Key-words: Craig and Gordon; deuterium; Dongmann; leaf water; leaf water enrichment; non-steady state; oxygen 18; Péclet; water isotopes.

Correspondence: M. Cuntz. Fax: +49 3641 57 7353; e-mail: mcuntz@bgc-jena.mpg.de

*Present address: Max-Planck-Institut für Biochemie, Jena, Germany.

†Present address: Smithsonian Tropical Research Institute, Republic of Panama.

INTRODUCTION

Leaf water isotope enrichment is a cornerstone of a variety of isotopic applications. Leaf water imprints the oxygen isotopic composition on different substances such as atmospheric CO_2 and O_2, and plant organic matter. This happens in different parts of the leaf and at different times. For example, leaf organic matter is formed in different intracellular compartments in the leaf so that the overall isotopic enrichment is thought to be more determined by bulk mesophyll water than by water at the evaporative sites (e.g. Barbour & Farquhar 2000; Cernusak *et al.* 2003). Leaf organic matter is mostly formed while there is energy input from photosynthesis so that the leaf organic matter reflects the assimilation-weighted average bulk mesophyll water enrichment. Atmospheric CO_2 and O_2, however, are probably determined by the isotopic composition of leaf water near the evaporating sites, at least in C_3 plants. Oxygen formation, for example, occurs at photosystem II, that is, in the chloroplasts, and the isotopic composition of the released oxygen is therefore close to the leaf water enrichment at the evaporative sites (Hill 1965; Helman *et al.* 2005). Water is only split in photosystem II, and oxygen evolved, if there is photosynthesis. The distribution of atmospheric oxygen isotopologues (cf. Dole effect, e.g. Bender, Sowers & Labeyrie 1994) is therefore determined by the electron transport-weighted average leaf water enrichment at the evaporative site. Atmospheric CO_2, however, can enter the leaf through the stomatal pores, exchange its isotopic composition with leaf water at the evaporative sites and exit the leaf through the stomatal pores again (Farquhar *et al.* 1993). This process occurs if stomata are open, regardless of whether there is photosynthesis or not. The isotopic composition of oxygen in atmospheric CO_2 is therefore determined by the leaf water enrichment at the evaporative sites weighted by the product of stomatal conductance and the CO_2 mixing ratio in the sub-stomatal cavity (one-way CO_2 flux from the stomata to the atmosphere) (Cernusak *et al.* 2004). Thus, it is essential to understand the time course of leaf water enrichment at both the evaporating sites and in the leaf mesophyll in order to harness the different isotopic signals.

Leaf water isotope enrichment is conventionally described by the steady-state Craig and Gordon equation (Craig & Gordon 1965 and Appendix B, Craig and Gordon model)

$$R_C = \alpha^+ \alpha_k (1-h) R_s + \alpha^+ h R_v, \quad (1)$$

where R_s is the isotopic ratio of plant available source water; R_v is the water vapour isotope ratio; α^+ (>1) is the equilibrium fractionation factor between liquid water and water vapour; α_k (>1) is the total kinetic fractionation factor associated with diffusion, and $h = w_a/w_i$ is the relative humidity corrected to leaf temperature, where w_i and w_a (mol mol^{-1}) denote air moisture in the stomatal cavity and in ambient air, respectively.

A number of studies have reported that observed leaf water is less enriched than the prediction of the steady-state Craig and Gordon equation, even after removing the unenriched veins before the measurements (e.g. Leaney *et al.* 1985; White 1989; Yakir, Deniro & Rundel 1989; Bariac, Jusserand & Mariotti 1990; Flanagan, Bain & Ehleringer 1991; Flanagan, Comstock & Ehleringer 1991; Flanagan 1993; Wang, Yakir & Avishai 1998; Roden & Ehleringer 1999). The cause of this observation is thought to relate to the following two explanations: (1) the leaf represents a continuum or a combination of unenriched (source) and enriched (evaporative sites) water, and (2) the steady-state assumption of the Craig and Gordon equation is only valid during certain periods of the day (e.g. midday) or over longer time scales, that is, days to weeks.

The former explanation has been termed the Péclet effect (Farquhar & Lloyd 1993): water isotopologues in the mesophyll are subject to advection from the xylem to the evaporative sites and back-diffusion of the enriched water at the evaporative sites to the xylem. The relative importance of advection and diffusion is characterized by a Péclet number $\wp$: if $\wp > 1$ advection is dominant and if $\wp < 1$ diffusion is the dominant transport process. Farquhar & Lloyd (1993) assigned the following Péclet number for advection–diffusion of water isotopes in leaves:

$$\wp_m = \frac{E L_{eff}}{C D}, \quad (2)$$

where E is transpiration rate (mol m^{-2} s^{-1}); D (m^2 s^{-1}) is the tracer diffusivity in liquid water; $C = 10^6/18 = 55.6 \cdot 10^3$ mol m^{-3} is the molar water concentration, and L_{eff} (m) is the effective length of water movement in the leaf mesophyll. The argument of Farquhar & Lloyd (1993) follows the idea outlined in Fig. 1a. The advection–diffusion in this picture happens along the path of the water molecules. Because of tortuosity of the water path through the mesophyll, the advection speed v along the path is k times greater than the slab velocity E/C, that is, $v = kE/C$. The effective length is therefore seen as k times the actual distance between the leaf xylem and the evaporative sites. In this picture and in the steady state, the mesophyll water isotope ratio increases exponentially from the xylem (R_s) to the Craig and Gordon value R_C at the evaporative sites. Bulk steady-state mesophyll water enrichment Δ_m^{ss} (expressed relative to source water) can then be written as

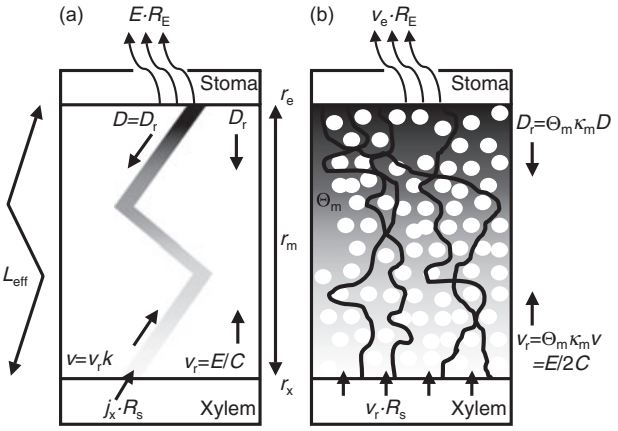

Figure 1. Idealized one-dimensional leaf geometry of (a) Farquhar & Lloyd (1993) and subsequent publications, and (b) of this study [and Ogée *et al.* (2007)]. The lower end of the inner box represents the interface between xylem and mesophyll (r_x), and the upper end represents the evaporating sites in the stomata (r_e). In (a), water isotopologues move along the grey tortuous path with advection velocity kE/C and diffusivity D. An isotopic gradient builds individually in each tortuous path, that is, individual paths are independent of each other. In (b), water moves along different tortuous paths (black lines) that cross and intermingle. The isotope gradient builds effectively in the r-direction (grey shading, darker means more enriched), with velocities reduced by tortuosity factor κ_m and volumetric mesophyll water content Θ_m. White circles represent air spaces that lead to $\Theta_m < 1$. The figure thus represents a conceptualization of the difference between the present modelling approach and that proposed previously by Farquhar & Lloyd (1993). Refer to Appendix A for definition of symbols.

$$\Delta_m^{ss} = \Delta_C \frac{1 - e^{-\wp_m}}{\wp_m} \quad (3)$$

with Δ_C the Craig and Gordon steady-state enrichment expressed relative to source water (i.e. Eqn 1 expressed relative to source water R_s).

Regarding the second explanation mentioned earlier, a non-steady-state leaf water enrichment model was first presented by Dongmann *et al.* (1974). By taking fixed environmental conditions between subsequent measurements, they found an iterative solution to compute leaf water enrichment over the diurnal course. However, Dongmann *et al.* (1974) and subsequent publications (Bariac *et al.* 1994; Cernusak, Pate & Farquhar 2002) did not distinguish between bulk leaf (mesophyll) water enrichment and enrichment at the evaporative sites. [In the following, we refer to this model as the Dongmann *et al.* (1974) non-steady-state model, but actually use the more rigorous formulation of Bariac *et al.* (1994).]

Farquhar & Cernusak (2005) combined both approaches in a non-steady-state model of bulk mesophyll water enrichment. They distinguished between bulk mesophyll water isotopic enrichment and enrichment at the evaporative sites, and they did not assume isotopic steady state. However, the model still contains a variety of assumptions. The model assumes, for example, that there is an exponential profile in the isotope ratio from the xylem to the evaporating sites and that this exponential profile has the same form as in steady state (Eqn 3 or cf. Eqns A14–A16). Another assumption is that a single effective mixing length L_{eff} describes the movement of water isotopes through the leaf mesophyll. Yet the leaf veins are generally in the middle of the leaf and, at least in amphistomatous leaves, there are two evaporative sites, one on each side of the leaf. So, there should be two isotope gradients in leaves, one at the adaxial (upper) side and one at the abaxial (lower) side. The measured mesophyll water enrichment Δ_{m} is then the water volume ($V_{\mathrm{m,up}}$, $V_{\mathrm{m,down}}$) weighted enrichment of both sides ($\Delta_{\mathrm{m,up}}$, $\Delta_{\mathrm{m,down}}$), that is, $\Delta_{\mathrm{m}} = (V_{\mathrm{m,up}}\Delta_{\mathrm{m,up}} + V_{\mathrm{m,down}}\Delta_{\mathrm{m,down}})/V_{\mathrm{m}}$. In steady state, this means that Eqn 3 should rather be

$$\Delta_{\mathrm{m}}^{\mathrm{ss}} = \Delta_{\mathrm{C}} \frac{V_{\mathrm{m,up}} \dfrac{1-e^{-\wp_{\mathrm{m,up}}}}{\wp_{\mathrm{m,up}}} + V_{\mathrm{m,down}} \dfrac{1-e^{-\wp_{\mathrm{m,down}}}}{\wp_{\mathrm{m,down}}}}{V_{\mathrm{m}}}, \tag{4}$$

which cannot be expanded to give a sensible combination of one single $\wp_{\mathrm{m}}$ or L_{eff}. This equation becomes that of Farquhar & Lloyd (1993) (Eqn 3) for leaves with a symmetrical cross-section (e.g. wheat). A third and maybe less critical assumption is that the tracer diffusivity D is constant. Yet it is shown in Appendix B (Diffusivity D) that the temperature dependence of D is significant.

We present here a description of advection and diffusion of water isotopologues in leaves that allows us to test some of the underlying assumptions of the Farquhar & Cernusak (2005) non-steady-state model. It is conceptually similar to the Péclet description, in that it assumes that water isotopologues are subject to advection and diffusion. We further compare the advection–diffusion model to observations and to other existing models in order to test the circumstances under which assumptions and simplifications are appropriate. A description of the advection–diffusion model is given subsequently. Following the model description, we explain how the current model relates to previously articulated models of leaf water enrichment. We begin the discussion of the model results with a detailed account of how the model was parameterized. We then discuss the predictive capability of the model with regard to both bulk leaf water isotopic enrichment and enrichment at the sites of evaporation in leaves. Next, we present a sensitivity analysis, focusing on model parameters that were assumed, but that could potentially be measured in future investigations. Finally, we discuss the implications of the current modelling approach for the various applications of leaf water enrichment that we detailed earlier.

MODEL DESCRIPTION

We describe water transport in the leaf mesophyll in a similar way to that for saturated soils (Zimmermann, Ehhalt & Münnich 1967). This is outlined in Fig. 1b. Water enters the mesophyll at $r = r_{\mathrm{x}}$, moves along tortuous paths and finally transpires at $r = r_{\mathrm{e}}$. These tortuous paths cross each other and mix their isotopic composition so that an effective gradient develops between the xylem and the evaporating sites. This is described by the advection–diffusion equation for porous media with an effective advection velocity v_r and an effective diffusivity D_{r} (cf. Ogée *et al.* 2007).

Advection–diffusion equation

Water moves from the xylem to the evaporating sites. Any tracer in the water is thus transported by advection with the effective water velocity v_{r}. If the tracer concentration χ is higher at one point compared with another, diffusion tries to adjust this imbalance. Diffusion is therefore an opposing effect that is proportional to the tracer concentration gradient (henceforth referred to as back-diffusion). The flux of a tracer at a certain point can thus be written as

$$J_{\mathrm{r}} = v_{\mathrm{r}}\chi - D_{\mathrm{r}}\frac{\partial \chi}{\partial r}. \tag{5}$$

The local continuity equation is then

$$\frac{\partial(\Theta_{\mathrm{m}}\chi)}{\partial t} = -\frac{\partial J_{\mathrm{r}}}{\partial r} = -\frac{\partial}{\partial r}\left(v_{\mathrm{r}}\chi - D_{\mathrm{r}}\frac{\partial \chi}{\partial r}\right). \tag{6}$$

We first take for χ the molar water concentration of $H_2{}^{16}O$ molecules, which is the most abundant isotopologue and whose concentration C is constant and uniform. We also take the volumetric water content Θ_{m} as uniform over the mesophyll. This implies that it changes simultaneously in the whole mesophyll, which is likely a simplification of reality. For example, a sharp increase in transpiration leads to an advection front that moves from the sites of evaporation to the xylem. However, the associated time constant is around 1 min, and it is therefore appropriate in this context to neglect this effect (Proseus, Ortega & Boyer 1999; Passioura & Munns 2000). This leads to

$$\frac{\partial \Theta_{\mathrm{m}}}{\partial t} = -\frac{\partial v_{\mathrm{r}}}{\partial r}. \tag{7}$$

If the volumetric water content Θ_{m} does not change with time (hydraulic steady state), the water velocity v_{r} in the mesophyll is uniform, that is, $v_{\mathrm{r}}(r,t) = v_{\mathrm{r}}(t)$.

Identifying now χ with the molar water concentration of $H_2{}^{18}O$ (or HDO) molecules, which, at natural abundance, can be expressed as $\chi = RC$, leads to

$$\frac{\partial(\Theta_{\mathrm{m}}R)}{\partial t} = -\frac{\partial(v_{\mathrm{r}}R)}{\partial r} + D_{\mathrm{r}}\frac{\partial^2 R}{\partial r^2}. \tag{8}$$

Combining both Eqns 7 and 8 gives the advection–diffusion equation in porous media:

$$\frac{\partial R}{\partial t} = -\frac{v_r}{\Theta_m}\frac{\partial R}{\partial r} + \frac{D_r}{\Theta_m}\frac{\partial^2 R}{\partial r^2}. \quad (9)$$

The effective diffusivity D_r is thereby related not only to the tracer diffusivity in liquid water D but also to the tortuosity factor κ_m (<1) of the water path through the mesophyll and the volumetric water content in the leaf mesophyll Θ_m (<1): $D_r = \Theta_m \kappa_m D$ (Shurbaji & Phillips 1995; Melayah, Bruckler & Bariac 1996). The effective velocity v_r will be treated in the next section.

Boundary conditions

The boundary condition for the continuity equation of $H_2{}^{16}O$ molecules (Eqn 7) is that of the velocity at the evaporating sites $v_r(r_e,t) = v_e(t)$. The effective advection velocity v_r is usually not uniform along the r-axis. It is, however, uniform when hydraulic steady state is reached, that is, leaf water volume is not changing anymore. In hypostomatous leaves v_r is then equal to the slab velocity E/C, and it is about half of the slab velocity in amphistomatous leaves: $E/2C$. This is because E is usually expressed relative to one-sided leaf area, regardless of the distribution of stomata over the leaf surface. The velocity profile in the mesophyll is thus (solution of Eqn 7)

$$v_r(r,t) = v_e(t) + \frac{\partial \Theta_m}{\partial t}(r_e - r) \qquad r \in [r_x, r_e]. \quad (10)$$

The volumetric water content in the leaf mesophyll Θ_m is simply related to the water volume V_m (per unit leaf area) and the mesophyll thickness $r_m = r_e - r_x$ through $\Theta_m = V_m/Cr_m$. The mesophyll water volume V_m changes with time, and so does volumetric water content Θ_m and/or the distance to the evaporative sites r_e. Changing dimensions (r_e) are difficult to deal with in numerical simulations. Because the observed quantity is mesophyll water volume V_m rather than leaf thickness, one can simulate the change in water volume solely by a change in volumetric water content Θ_m, fixing the spatial dimensions r_e, r_x and hence r_m, that is, $V_m \propto \Theta_m$. This workaround should have, however, negligible influence because the Péclet number $\wp_m$ is the same if one includes variable dimensions or solely changes volumetric water content Θ_m. Hence, the velocity profile in the mesophyll can be written as

$$\frac{v_r(r,t)}{\Theta_m} = \frac{E}{2C\Theta_m} + \frac{1}{V_m}\frac{\partial V_m}{\partial t}(r_e - r) \qquad r \in [r_x, r_e], \quad (11)$$

with the velocity at the evaporating sites $v_r(r_e,t) = v_e(t)$ equal to $E/2C$ for amphistomatous leaves. This shows the influence of changing leaf water status and that the water velocity in the mesophyll is uniform ($E/2C$) if mesophyll water volume V_m is constant.

The boundary conditions for the continuity equation of $H_2{}^{18}O$ molecules (Eqn 9) are given by the continuity of the flux. The water isotope flux that enters the mesophyll from the xylem must equal $v_r(0,t)R_s$, and the water isotope flux that leaves the stomata must equal $v_e(t)R_E$:

$$v_r(r_x,t)R(r_x,t) - D_r\left.\frac{\partial R}{\partial r}\right|_{r_x,t} = v_r(r_x,t)R_s \quad (12)$$

$$v_e(t)R(r_e,t) - D_r\left.\frac{\partial R}{\partial r}\right|_{r_e,t} = v_e(t)R_E(t). \quad (13)$$

The last equation can be rewritten as [with $v_e(t) = E/2C$ and Eqn A3]:

$$\frac{E}{2C(1-h)}\left[1 - h - \frac{1}{\alpha_k \alpha^+}\right]R(r_e,t) - D_r\left.\frac{\partial R}{\partial r}\right|_{r_e,t} = -\frac{E}{2C(1-h)}\frac{h}{\alpha_k}R_v. \quad (14)$$

Note that as $h \to 1$, $E/(1-h)$ must be replaced by $g_t w_i$.

Remarks

For amphistomatous leaves with an asymmetric cross-section, like most dicotyledonous leaves with palisade cells on the adaxial side and spongy mesophyll on the abaxial side such as tobacco or spinach leaves, Θ_m and κ_m should be different on each side of the leaf, even with an equally distributed stomatal density. The mesophyll thickness r_m is also likely to be different. The advection–diffusion model can take this effect into account by solving two separate advection–diffusion equations (one for each side of the leaf) and then averaging the leaf water enrichment, weighted by water volume.

There are still potentially a variety of complications in leaves that do not allow such a simplified description of leaf water isotope enrichment. Effects such as hydrodynamic and mechanical dispersion should be negligible in this context with the relevant advection speeds (Passioura 1971; Gvirtzman & Gorelick 1991).

Other effects such as isotopic transport in the vapour phase instead of the liquid phase may not be negligible, though, because tracer diffusivity in the vapour phase is about 10^5 higher than that in the liquid phase. However, the vapour molar concentration is also about 10^5 smaller in the vapour compared with liquid water so that the diffusive flux should be similar in the vapour and in liquid phases.

Finally, it is the current understanding that there are three parallel pathways for liquid water movement in leaves: symplastic (through the plasmodesmata), transcellular (across cell membranes via aquaporins) and apoplastic (along cell walls), with $\kappa_{symplastic} < \kappa_{apoplastic} < \kappa_{transcellular}$ (Barbour & Farquhar 2004). It is very possible that the relative importance of these three pathways for total water movement varies with transpiration rate E. For example, a high transpiration rate will most likely thin the water film along cell walls and diminish the influence of the apoplastic pathway. However, we take κ_m to be constant because the

study of water movement in plants is not sufficiently advanced to allow such a partitioning. We do, however, emphasize that it is likely that κ_m changes with time and environmental conditions.

Relationships with previous models and model limitations

We show in Appendix B [Relating advection–diffusion to Farquhar & Lloyd's (1993) steady-state Péclet effect] that the advection–diffusion equation (Eqn 9) leads directly to the steady-state model of Farquhar & Lloyd (1993) (Eqn 3). This is evident because the advection–diffusion equation is simply the generalization of the Farquhar and Lloyd steady-state Péclet formulation to non-steady state. However, Farquhar & Lloyd (1993) use a constant effective length L_{eff} because they are in steady state. We do not consider L_{eff} to be constant here but define it as $L_{eff} = r_m/2\Theta_m\kappa_m$ (i.e. $k = 2/\Theta_m\kappa_m$). Θ_m obviously changes with leaf water volume so that L_{eff} is changing because of the leaf water volume change but becomes constant in steady state.

We also show in appendix B [Relating advection–diffusion to the Farquhar & Cernusak (2005) non-steady-state model] that the advection–diffusion equation (Eqn 9) conforms to the mass-budget derivation of Farquhar & Cernusak (2005). However, it does not assume the form of the isotope gradient from the xylem to the evaporative sites but rather calculates this gradient at any given time.

The present model does not take into account varying source water R_s along the leaf length. Farquhar & Gan (2003) showed that accounting for this effect, which is prominent in long monocotyledon leaves, leads to an enriched bulk xylem water in the steady state ($\Delta_x^{ss} \neq 0$), but that the enrichment for bulk mesophyll water (Δ_m^{ss}) was still described by the Farquhar & Lloyd (1993) Péclet description (Eqn 3). Using a full two-dimensional treatment of advection and diffusion in leaf water, Ogée *et al.* (2007) have further shown that a bulk description of leaf water enrichment such as the one presented in Farquhar & Cernusak (2005) was still valid in non-steady state even in long monocotyledonous leaves. The present one-dimensional advection–diffusion description is of intermediate complexity between the bulk ('zero-dimensional') model of Farquhar & Cernusak (2005) and the two-dimensional treatment of Ogée *et al.* (2007). It can be derived from the Ogée *et al.* (2007) model for constant leaf water volume V_m by assuming a well-mixed uniform xylem isotope ratio R_s. However, the present model also treats changing leaf water volume V_m and can deal with asymmetric leaf cross-sections, which were not implemented in Ogée *et al.* (2007).

We believe that our model is well adapted to amphistomatous leaves. Our model is less well adapted to needles because water movement is then better described by a radial symmetry along the needle axis rather than by the planar symmetry adopted here (Eqn 5 *et seqq*.). To treat this case, the model of Ogée *et al.* (2007) could be used because it already includes a radial description of xylem water movement that can easily be expanded to the mesophyll. The present model is probably not well adapted to hypostomatous leaves either. Indeed hypostomatous leaves have two distinctively different leaf sides: one side gets enriched directly by evaporation, and the other side gets enriched only by diffusion. There may be advection in the stomata free side as well, especially when leaf water status changes, but it is most probably possible to treat the adaxial site as a water buffer reservoir with no advection but diffusion. This would lead to two coupled advection–diffusion equations (one having no advection) and is beyond the scope of this study.

Numerical solution

The numerical model discretizes the advection–diffusion equation for porous media, Eqn 9, including the boundary conditions, Eqns 12 and 14. For that, the velocity profile $v_r(r,t)$ is first calculated, according to Eqn 11, and using measured values of mesophyll water content $\Theta_m(t) = V_m(t)/Cr_m$.

Two advection–diffusion equations, one for the adaxial and one for the abaxial leaf side, are solved numerically with an algorithm implicit-backward in time and centred in space, which is unconditionally stable, that is, independent of step sizes in time and space. We took a 10 min time step and a 1 μm resolution in the r-direction.

We arbitrarily take the first measured value as initial condition everywhere in the leaf.

RESULTS AND DISCUSSIONS

Model parameterization

We applied the advection–diffusion model to two independent data sets of *Lupinus angustifolius* (Cernusak *et al.* 2002) and *Eucalyptus globulus* (Cernusak, Farquhar & Pate 2005). Both species are amphistomatous dicotyledons. The adaxial and abaxial parts of the leaf have different leaf geometries and thus, for example, different volumetric water contents Θ_m. The adaxial (upper) and abaxial (lower) leaf parameters for the two advection–diffusion equations were estimated for lupin from cross-sections of typical dicotyledonous leaves (e.g. Atwell, Kriedemann & Turnbull 1999) and were taken from James & Bell (2001) for Tasmanian blue gum (see Appendix B, Leaf parameters for the adaxial and abaxial leaf sides). Because of lack of knowledge about water flow in the mesophyll, we assumed the same tortuosities in the adaxial and abaxial leaf parts, that is, $\kappa_{m,up} = \kappa_{m,down} = \kappa_m$. But we emphasize that the relative importance of the above-mentioned three water pathways (symplastic, transcellular, apoplastic) could be, and probably is, different in the adaxial and abaxial part of the leaf, so that $\kappa_{m,up}$ and $\kappa_{m,down}$ are most probably different. With these estimates, all the relevant parameters can be calculated from the measured intermediate effective length L_{eff} and mesophyll water volume V_m (the values of the parameters and details of the calculations are given in

Appendix B, Leaf parameters for the adaxial and abaxial leaf sides). If one cannot estimate the leaf parameters mentioned earlier, we suggest using the observed L_{eff} and V_m to calculate one single advection–diffusion equation, which is equivalent to a symmetric cross-section. However, one still has to measure/estimate leaf thickness to get Θ_m from the water volume V_m.

The effective lengths L_{eff} in the original publications were estimated with a fixed value of $D = 2.66{\cdot}10^{-9}$ m^{-2} s^{-1} for $H_2{}^{18}O$, which would correspond to a leaf temperature of 32.5 °C (see Appendix B, Diffusivity D). This leaf temperature would be 5–10° higher than the maximum daytime temperature in the data sets. However, the 'real' tortuosity κ_m is not known for any species, and κ_m or L_{eff} are pure fitting parameters. We show the sensitivity to L_{eff} of the advection–diffusion model in Fig. 3c and discuss it in the next section. For *L. angustifolius*, we took as standard L_{eff} the values of Farquhar & Cernusak (2005) corrected to D of the mean midday temperature of ca. 25 °C ($D = 2.2{\cdot}10^{-9}$ m^{-2} s^{-1}): $L_{eff} = 12$ mm (using the fractionation factors of Cappa *et al.* 2005) and 7 mm (using the fractionation factors of Merlivat 1978), respectively. We took the standard L_{eff} for *E. globulus* so that the advection–diffusion model with constant mesophyll water volume V_m best fitted the observations: $L_{eff} = 60$ mm (with Cappa *et al.* 2005) and 50 mm (with Merlivat 1978). We show in the following results obtained with Merlivat's fractionation factors. Results for lupin $\Delta^{18}O$ and blue gum $\Delta^{18}O$ are basically identical to the results obtained with Cappa *et al.* (2005) because of the adapted L_{eff}. However, using Cappa *et al.* (2005) in the case of lupin Δ^2H leads to Craig and Gordon steady-state estimates that are lower than the measured mesophyll bulk water enrichment. This comes most probably from the fact that vapour isotopes were not measured but taken to be constant at the mean value of Perth, Western Australia (Rich 2004). This underlines the importance of measuring water vapour isotopes.

Bulk mesophyll enrichment Δ_m

Figure 2 shows the comparison between measured and modelled Δ_m. It compares the advection–diffusion model calculated independently for the adaxial and abaxial sides (named '2m' for two mesophylls) with the observations, and also with the Farquhar & Cernusak (2005) non-steady-state model and an advection–diffusion model for a symmetrical leaf, that is, the adaxial and abaxial sides are the same (named '1m' for one mesophyll). It is noticeable that the advection–diffusion model is less sensitive to noise in the input data and gives smoother results than the Farquhar & Cernusak (2005) non-steady-state model. A perturbation in the input data has to propagate from the evaporative sites throughout the mesophyll in the advection–diffusion model, whereas it acts instantaneously on the whole mesophyll in the Farquhar & Cernusak (2005) non-steady-state model. It is also apparent that taking just one single set of leaf parameters (1m) performs equally satisfactorily as making the distinction between adaxial and abaxial sides. There is even no apparent difference between 2m and 1m in the case of Tasmanian blue gum. However, this depends strongly on the morphological and physiological differences between the adaxial and abaxial sides. Figure 3a shows the two independent advection–diffusion models for $\Delta^{18}O_m$ of both leaf sides of lupin, and the weighted mean. Figure 3b shows the same model results calculated with extreme and unrealistic differences between adaxial and abaxial sides, that is, close to 90% of the water volume is in the adaxial side, whereas it is only ca. 65% in the standard case. One can see that the weighted mean is heavily biased towards the adaxial side, and it compares quite favourably still with the observations in the extreme case. But the water volume in the adaxial side is too big in the extreme case in order for the mesophyll water to descend to the steady-state value during night. This strongly depends on the night-time stomatal conductance $g_{s,night}$. This was not measured for either of the data sets, and standard values were taken in the original publications (Cernusak *et al.* 2002, 2005). We took the same values as in the original publications but show the sensitivity of the lupin $\Delta^{18}O_m$ values to $g_{s,night}$ in Fig. 3d. This shows that there has to be a non-zero stomatal conductance at night; otherwise, the mesophyll water would only relax to its mean isotopic composition just before the stomata closed. This exposes the night-time stomatal conductance to be a mere additional fitting parameter if it is not measured, as is the case in our data sets. Figure 3c shows the sensitivity of the lupin $\Delta^{18}O_m$ values to L_{eff}. L_{eff} is important mostly during the day, while $g_{s,night}$ is determinant during the night. One has, in summary, two fitting parameters, L_{eff} to get the amplitude of Δ_m right and $g_{s,night}$ to get the right time course of Δ_m during the night.

Both oxygen (Fig. 2a) and deuterium (Fig. 2b) isotopes were measured in *L. angustifolius*, and they follow the same diurnal cycle and are both well fitted with the same chosen L_{eff} and $g_{s,night}$. This indicates that there is at least some physical reality in the approach of enriched non-steady-state leaf water with influx of unenriched vein water. It does, however, neither support nor disprove the Péclet effect because one can get comparably good results by taking different well-mixed metabolic pools of water (Yakir 1997, results not shown).

Enrichment at the evaporative sites Δ_e

The isotopic composition of atmospheric O_2 and CO_2 are probably influenced by leaf water close to the evaporating sites Δ_e rather than by bulk mesophyll water Δ_m, at least in C_3 plants. One can calculate the enrichment at the evaporative sites Δ_e from the change in time of observed bulk leaf mesophyll water Δ_m (cf. Eqn A9 and Harwood *et al.* 1998). Figure 4 shows the isotopic compositions at the evaporative sites Δ_e predicted from the measured bulk mesophyll water isotopic compositions Δ_m. The derived values at night depend strongly on the measurements of mesophyll water volume V_m, at least for Tasmanian blue gum, which are very noisy because they were measured at leaves adjacent to the leaves of the gas exchange and isotope measurements. We

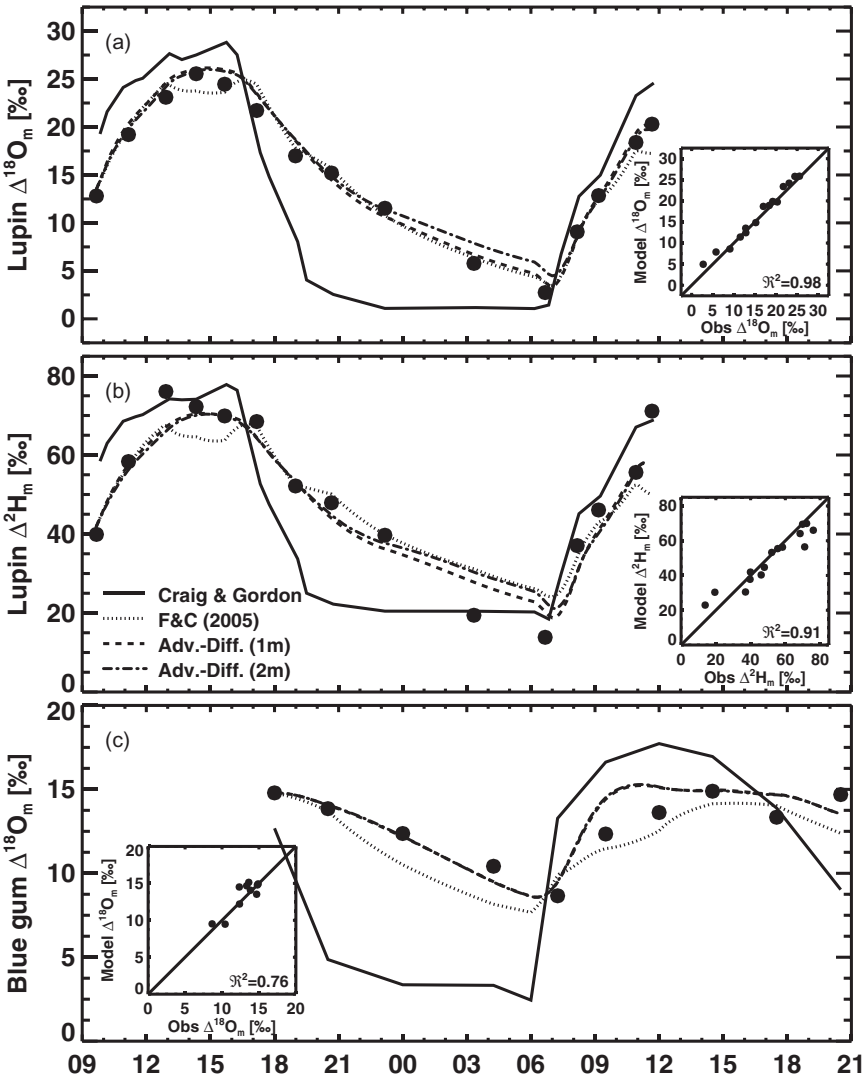

Figure 2. Validation of the present model with observations of the diurnal course of bulk mesophyll enrichment Δ_m of lupin ^{18}O (a), lupin ^{2}H (b) and blue gum ^{18}O (c). Filled circles are observations, and lines represent the Craig and Gordon steady-state prediction (solid), the Farquhar & Cernusak (2005) non-steady-state model [dotted, F&C (2005)], the advection–diffusion model for a symmetric leaf [dashed, adv.-diff. (1m)], and the advection–diffusion description with different adaxial and abaxial leaf sides [dash dot, adv.-diff. (2m)]. The insets are the predictions of the full advection–diffusion model [adv.-diff. (2m)] and the observed leaf water enrichments. The line is the 1:1 line and the coefficient of determination $\Re^2$ between model and data is given. The figure illustrates the predictions of the advection–diffusion model in relation to observations and to predictions of previous leaf water models. Refer to Appendix A for definition of symbols.

therefore plotted also the derived values of Δ_e with constant mean leaf water volume V_m. We compared the derived values of Δ_e to the symmetric advection–diffusion model (1m) and to the Farquhar & Cernusak (2005) non-steady-state model, but taking a mean leaf water volume V_m. We also included the Dongmann *et al.* (1974) non-steady-state model, which does not distinguish between bulk leaf water and leaf water at the evaporative sites and takes a mean leaf water volume as well. All models are quite similar and perform very well during the day because both data sets reach steady state during early afternoon. This can be tested more critically on leaves with higher leaf water volumes such as needles (Seibt *et al.* 2006). All models perform well for the whole diurnal cycle of lupin. There are notable differences at night that can be caused by missing atmospheric water vapour isotope measurements. Water vapour isotopic composition for lupin was assumed constant at the mean value for Perth, Western Australia (Rich 2004). However, water vapour isotopes were measured in the blue gum experiment and did not improve the comparison between the models and the derived values. The model values seemed not to decrease enough during the night to explain the derived values. This would indicate that the night-time stomatal conductance could be larger (independent of the Péclet effect), but this would lead to great discrepancies in the Δ_m values.

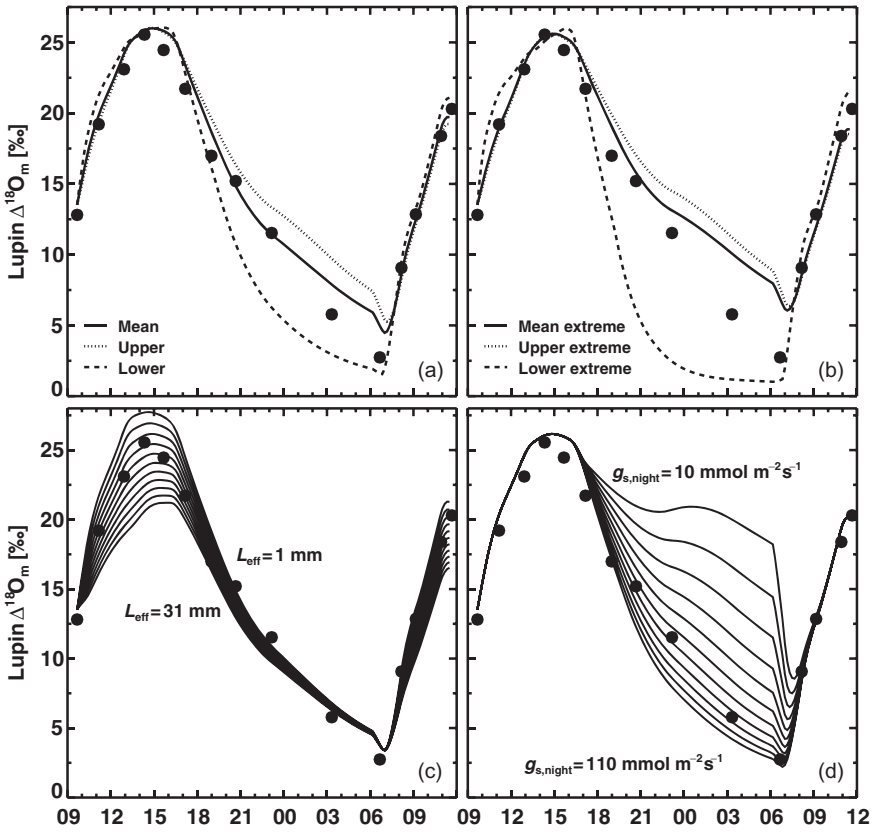

Figure 3. Sensitivity of the bulk mesophyll enrichment $\Delta^{18}O_m$ of lupin in the advection–diffusion model. (a) The two individual advection–diffusion models for the adaxial (dotted, upper) and the abaxial (dashed, lower) sides and the water volume weighted mean (solid, mean). (b) Same as (a), but with extreme estimates of leaf geometry for the adaxial and abaxial sides. (c) Sensitivity of the symmetric advection–diffusion model to different effective lengths L_{eff} (10 lines equally spaced between L_{eff} = 1 mm and L_{eff} = 31 mm). (d) Sensitivity of the symmetric advection–diffusion model to different night-time stomatal conductances $g_{s,night}$ (10 lines equally spaced between $g_{s,night}$ = 10 mmol m^{-2} s^{-1} and $g_{s,night}$ = 110 mmol m^{-2} s^{-1}). The four panels illustrate therefore the sensitivity of the advection–diffusion model to key parameters. Refer to Appendix A for definitions of symbols.

It is noteworthy that the Dongmann *et al.* (1974) non-steady-state model performs as well as the other models for Δ_e, which indicates that leaf water volume V_m measurements are not very crucial observation for Δ_e. The Dongmann *et al.* model is normally used in global models of $\delta^{18}O$ in atmospheric CO_2 (Cuntz *et al.* 2003). But this has to be confirmed, for example, at species with higher leaf water volumes that do not reach steady-state during midday, such as needles (Lai *et al.* 2006; Seibt *et al.* 2006).

Sensitivity analysis

We performed a variety of sensitivity analyses to assumptions and methods that are used in other leaf water enrichment models: (1) symmetric cross-section of leaf (1m), (2) constant diffusivity at certain leaf temperatures D(°C), (3) constant mesophyll water volume $V_{m,const}$, (4) same isotopic gradient in non-steady state as in steady state (Farquhar & Cernusak 2005), (5) solving algorithms (Dongmann-style, Excel Solver). The sensitivity runs are summarized in the form of Taylor diagrams in Fig. 5. The Taylor-diagram (Taylor 2001) shows in polar coordinates the correlation coefficient $\Re$ and the normalized standard deviation (SD) $\hat{\sigma}$ of sensitivity runs versus standard model run (advection–diffusion, 2m). The point at unit distance from the origin along the abscissa is the reference point where a perfect model–model match would be situated. In summary, the correlation coefficient $\Re$ gives information about the right phasing (the better the phasing, the closer is the symbol to the abscissa), and the normalized SD $\hat{\sigma}$ gives information about the amplitude of the sensitivity run compared to the standard model (the better the amplitudes agree, the closer the symbol is to the dashed line of unity in Fig. 5). We show here rather a model versus model than a model versus data comparison because of the two fitting parameters L_{eff} and $g_{s,night}$, which were chosen so that one particular model performs best compared with the observations. For example, in the case of Tasmanian blue gum, L_{eff} and $g_{s,night}$ were chosen with the symmetrical advection–diffusion model (1m) with a fixed mean water volume $V_{m,const}$ (filled standing hourglass), which consequently performed best among the model runs compared with the observations.

In all three cases (lupin $\Delta^{18}O_m$, lupin Δ^2H_m and blue gum $\Delta^{18}O_m$), the advection–diffusion model shows slightly less sensitivity than the Farquhar & Cernusak (2005) non-steady-state model. As already stated earlier, the advection–diffusion model performs similarly in the case of two distinct leaf halves (standard model, 2m) and with symmetric leaf halves (filled square, 1m), that is, the symmetric advection–diffusion model or filled square is very close to the point of unity at the abscissa. The Farquhar & Cernusak (2005) non-steady-state model (open square) is also very similar in the case of lupin, but deviates substantially in the case of blue gum. This comes from the slightly different sensitivities of the advection–diffusion and the Farquhar & Cernusak (2005) non-steady-state models to leaf water volume V_m changes. The hourglasses show the models' sensitivity to fixed water volume V_m. Apparently, both the advection–

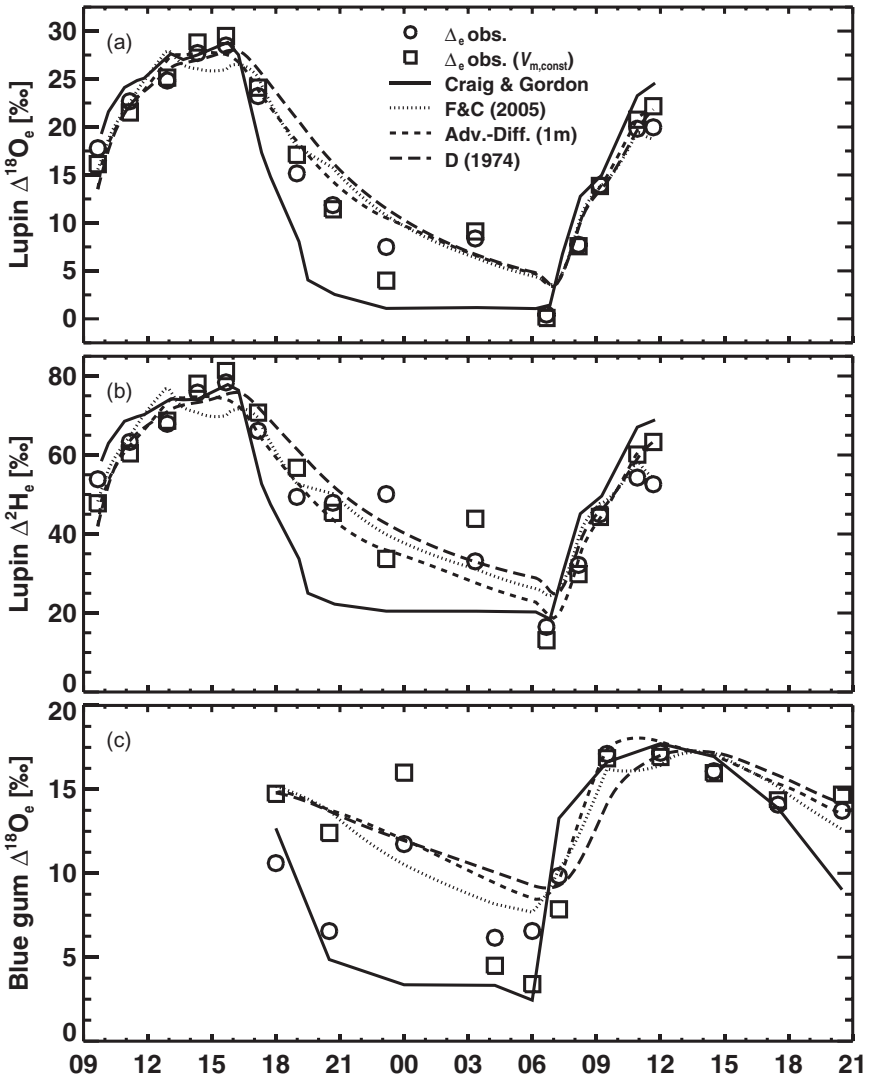

Figure 4. Model performance at the sites of evaporation Δ_e compared to derived diurnal courses of Δ_e of lupin ^{18}O (a), lupin ^{2}H (b) and blue gum ^{18}O (c). Open circles are derived from observations of bulk mesophyll water enrichment Δ_m and mesophyll water volume V_m, while open squares are derived from the same observations of Δ_m but with a mean observed water volume V_m. Lines represent the Craig and Gordon steady-state (solid), the Farquhar & Cernusak (2005) non-steady-state [dotted, F&C (2005)], the symmetric advection–diffusion [dashed, adv.-diff. (1m)] and the Dongmann *et al.* (1974) non-steady-state [D (1974)] models. The figure illustrates predictions of Δ_e by the advection–diffusion model and previous models in relation to calculated values for Δ_e, which are based on observations of mesophyll leaf water enrichment and leaf water content. Refer to Appendix A for definition of symbols.

diffusion and Farquhar & Cernusak (2005) non-steady-state models are very similar with fixed mean leaf water volume V_m (standing hourglasses). The models show an influence of mesophyll water volume V_m on amplitude and phase. If the water volume V_m taken is too high, the leaf water enrichment Δ_m decreases too slowly during the night, whereas a low water volume V_m leads to a decrease of leaf water enrichment Δ_m at night, which is too rapid. However, there is interplay between night-time stomatal conductance $g_{s.night}$ and leaf water volume V_m because the time constant for leaf water enrichment changes is proportional to $V_m/g_t w_i$ [cf. Appendix B, Solution to the Farquhar & Cernusak (2005) and earlier non-steady-state models]. But if night-time stomatal conductance $g_{s,night}$ is measured, it becomes essential to get a realistic estimate of the mean leaf water volume V_m. It is impossible to determine with our data sets how important it is to measure leaf water volume changes during the day. Our data sets indicate that a mean leaf water volume $V_{m,const}$ is sufficient, but measuring water volume can be more important if night-time stomatal conductance $g_{s,night}$ is measured.

The half circles show the models' sensitivities to fixed diffusivities D at different temperatures. The diffusivity D is most important during daytime so that the models show most sensitivity in the amplitude rather than the phase. An erroneous diffusivity D can bias the model results by up to 10% (e.g. Fig. 5c).

The Farquhar & Cernusak (2005) non-steady-state model was solved with a fourth-order Runge–Kutta algorithm (e.g.

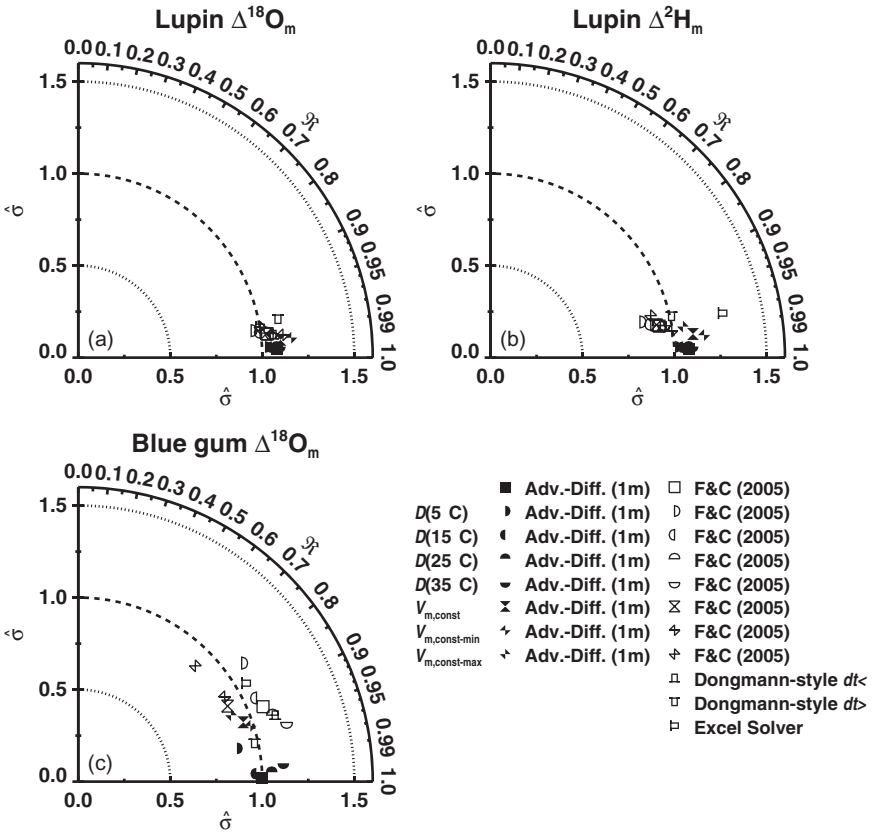

Figure 5. Sensitivity of modelled bulk mesophyll enrichment Δ_m (Adv.-Diff. 2m) of lupin ^{18}O (a), lupin ^{2}H (b) and blue gum ^{18}O (c) to assumptions and methods that are used in other leaf water model descriptions. The polar diagrams show the normalized SD $\hat{\sigma}$ of the model runs (normalized to the full advection–diffusion model SD) in radial direction and the correlation coefficient $\Re$ between the full advection–diffusion model and the sensitivity run on the azimuth scale. Note that the circular $\Re$-axis is in inverse cosine (arccosine) scale (cf. Taylor 2001). Open symbols denote the Farquhar & Cernusak (2005) non-steady-state model [F&C (2005)], and closed symbols denote the advection–diffusion model, where '1m' stands for the symmetric advection–diffusion model with same leaf parameters for the adaxial and abaxial leaf sides. Half circles mark runs with fixed diffusivities D at different temperatures and hourglasses mark runs with fixed mesophyll leaf water volume V_m, where $V_{m,const}$ stands for the mean, $V_{m,const-min}$ for the minimum and $V_{m,const-max}$ for the maximum observed values in the data sets. Open hats mark different solving algorithms for the Farquhar & Cernusak (2005) non-steady-state model and are explained in the text. In summary, the aggregation or disaggregation of points on the charts shows the similarity or dissimilarity of model runs with respect to predictions of the full advection–diffusion model. Refer to Appendix A for definition of symbols.

Press *et al.* 1992). Dongmann *et al.* (1974) showed an iterative solution to their ordinary differential equation (ODE). To our knowledge, one can solve all published non-steady-state models of bulk leaf water enrichment with the same iterative solution [see Appendix B, Solution to the Farquhar & Cernusak (2005) and earlier non-steady-state models], which we call 'Dongmann-style solution'. This is strictly incorrect for the Farquhar & Cernusak (2005) non-steady-state model but the smaller the time step *dt*, the smaller the error in the iterative solution (cf. Appendix B, Solution to the Farquhar & Cernusak (2005) and earlier non-steady-state models). The Dongmann-style solution is appealing because of its simplicity and because it can be calculated in a simple spreadsheet. We included in Fig. 5 two Dongmann-style solutions of the Farquhar & Cernusak (2005) non-steady-state model, once calculated only at times of leaf water enrichment measurements (ca. 2–4 h apart, *dt*>, hat down) and once calculated in 10 min time steps (*dt*<, hat up). We also included the solution obtained with the Microsoft Excel Solver (hat right), as suggested by Farquhar & Cernusak (2005). Both Dongmann-style solutions perform as well as the more rigorous Runge–Kutta solution. There is no preference here whether Dongmann-style should be solved with small or large time steps. The Microsoft Excel Solver is in the range of the other sensitivity runs with a tendency to deviate from the Runge–Kutta solution. But our data sets indicate that the errors as a result of the solving algorithm are less important than other unknowns.

Applications of leaf water enrichment

Different applications of leaf water enrichment use enrichment in different parts of the leaf and weighted by different

	Weighting variable			
	Non	A	$g_t w_i$	$g_t C_i$
Δ_m adv.-diff.	14.6|44.7|12.9	17.3|50.5|14.7	16.1|47.9|14.2	12.7|40.2|13.9
Δ_m F&C (2005)	14.3|46.2|11.6	16.9|51.0|12.7	15.7|48.7|12.3	12.5|42.3|12.1
Craig and Gordon	11.1|40.8|09.9	18.9|57.1|16.6	17.2|53.4|15.2	12.4|43.5|14.0
Δ_e adv.-diff.	15.1|46.3|13.7	18.5|53.8|17.0	17.3|51.1|16.2	13.5|42.5|15.6
Δ_e F&C (2005)	15.2|48.9|12.9	18.6|56.2|16.1	17.3|53.7|15.3	13.6|46.0|14.8
Δ_e D (1974)	15.7|50.6|13.4	18.6|55.9|15.8	17.3|53.2|15.1	13.6|45.9|14.7

Table 1. Average weighted bulk mesophyll water enrichment Δ_m and enrichment at the evaporative sites Δ_e, relevant for different leaf water isotope applications, of the advection–diffusion description (adv.-diff.) compared to simpler leaf water enrichment models: the Farquhar & Cernusak (2005) non-steady-state [F&C (2005)], the Dongmann *et al.* (1974) non-steady-state [D (1974)] and the Craig and Gordon steady-state model

The weighting is by different gas exchange parameters for 1 day, where 'Non' stands for no weighting, A for assimilation, $g_t w_i$ for the one-way H_2O flux and $g_t C_i$ for the one-way CO_2 flux from the stomata into the atmosphere. The three values at each weighting are from left to right: lupin $\Delta^{18}O$, lupin Δ^2H and blue gum $\Delta^{18}O$.

fluxes: (1) leaf organic matter isotopic composition is determined by bulk mesophyll water Δ_m and, because it is mostly formed while there is energy input from photosynthesis, the leaf organic matter reflects the assimilation-weighted average bulk mesophyll water enrichment Δ_m; (2) molecular oxygen evolution from the leaf to the atmosphere is the electron transport-weighted leaf water enrichment at the evaporative sites Δ_e; (3) the isotopic composition of atmospheric CO_2 is determined by the $g_t C_i$ weighted average leaf water enrichment at the evaporative sites Δ_e, where C_i is the CO_2 mixing ratio in the stomatal air space; (4) the atmospheric water vapour receives the signal $E\Delta_E$, which is determined by the one-way isotope flux of H_2O from the leaf stomata into the atmosphere $g_t w_i \Delta_e$ (cf. Eqn A9). These different applications of leaf water enrichment are used from the leaf level up to global scales. It is therefore crucial to ask how much error one introduces by using a simpler model of leaf water enrichment such as the Craig and Gordon steady-state prediction or the Dongmann *et al.* (1974) non-steady-state model. We thus calculated 1 day averages of leaf water enrichment, weighted with different CO_2 and H_2O fluxes, shown in Table 1. Assimilation rate is closely linked to electron transport (Farquhar, von Caemmerer & Berry 1980) so that we take assimilation as a surrogate for electron transport.

All weighted averages are very different from the non-weighted averages, and they are also quite different from each other. The non-weighted averages lie in-between the assimilation weighted and the CO_2 one-way flux weighted averages. This would make a difference between leaf water isotopic composition relevant to atmospheric O_2 and that relevant to atmospheric CO_2 of ca. 5‰ in lupin and ca. 1.3‰ in blue gum. The discrepancy between global leaf water $\delta^{18}O$ estimates based on budget calculations of $\delta^{18}O$ in atmospheric CO_2 and $\delta^{18}O$ in atmospheric O_2 (Bender *et al.* 1994; Keeling 1995) can well be just a matter of different weightings (cf. Cernusak *et al.* 2004). The weighted averages of bulk mesophyll water Δ_m and water at the evaporating sites Δ_e are all very different, and the Craig and Gordon steady-state prediction is naturally closer to the evaporating sites Δ_e. Applications that involve bulk mesophyll water enrichment Δ_m (e.g. tree rings) therefore introduce a bias towards higher values while not taking the Péclet effect into account.

The Farquhar & Cernusak (2005) and the Dongmann *et al.* (1974) non-steady-state models are very similar in the averages of the enrichment at the evaporating sites Δ_e. So it would probably not be very important to take the Péclet effect into account in our data sets if we are not dealing with organic matter.

It is noteworthy that the model calculations with mean volumetric leaf water V_m deviate less than 0.5‰ in $\Delta^{18}O$ and less than 1‰ in Δ^2H from the calculations with varying leaf water (not shown).

CONCLUSIONS

We have developed an advection–diffusion description of water isotopologues in leaves, similar to Ogée *et al.* (2007). We have shown it underlies the Farquhar & Cernusak (2005) non-steady-state model. But the present model can deal with asymmetric leaf cross-sections and does not assume the shape of the isotopic gradient in non-steady state, contrary to the Farquhar & Cernusak (2005) non-steady-state model. The latter model shows more sensitivity to input parameters than the advection–diffusion description because the input parameters act on the whole mesophyll at once in the Farquhar & Cernusak (2005) non-steady-state model, whereas any change has to propagate first through the mesophyll in the advection–diffusion description. However, the Farquhar & Cernusak (2005) non-steady-state model performs equally well compared to observations given the uncertainties in the model parameters.

Night-time stomatal conductance $g_{s,night}$ is essentially a tuning parameter in our analysis (and also in the original publications) but could potentially be measured. Water transport in leaves is subject of considerable debate so that the effective length L_{eff} [in the Farquhar & Cernusak (2005) non-steady-state model] or the tortuosity factor κ_m (in the advection–diffusion model) are unknown and are therefore fitted parameters for the models. Measuring both $\delta^{18}O$ and δ^2H on the same leaves should however allow the uncertainty to be narrowed for estimates of L_{eff} or κ_m.

Our data sets together with the advection–diffusion model suggest that simpler leaf water enrichment models such as the Farquhar & Cernusak (2005) or the Dongmann *et al.* (1974) non-steady-state model or even the Craig and Gordon steady-state prediction might be sufficient in particular applications of leaf water enrichment if weighted with the appropriate fluxes.

ACKNOWLEDGMENTS

M. Cuntz is sponsored by a European Union Marie-Curie Fellowship (contract number MOIF-CT-2004-008087). G.D. Farquhar acknowledges support from the Australian Research Council.

REFERENCES

Atwell B.J., Kriedemann P.E. & Turnbull C.G.N., eds (1999) *Plants in Action: Adaptation in Nature, Performance in Cultivation* 1st edn. Palgrave MacMillan, Melbourne, Australia.

Barbour M.M. & Farquhar G.D. (2000) Relative humidity- and ABA-induced variation in carbon and oxygen isotope ratios of cotton leaves. *Plant, Cell & Environment* **23,** 473–485.

Barbour M.M. & Farquhar G.D. (2004) Do pathways of water movement and leaf anatomical dimensions allow development of gradients in $H_2{}^{18}O$ between veins and the sites of evaporation within leaves? *Plant, Cell & Environment* **27,** 107–121.

Bariac T., Gonzalezdunia J., Katerji N., Bethenod O., Bertolini J.M. & Mariotti A. (1994) Spatial variation of the isotopic composition of water (^{18}O, ^{2}H) in the soil-plant-atmosphere system. 2. Assessment under field conditions. *Chemical Geology* **115,** 317–333.

Bariac T., Jusserand C. & Mariotti A. (1990) Temporospatial development of the isotopic composition of water in the soil-plant-atmosphere continuum. *Geochimica Et Cosmochimica Acta* **54,** 413–424.

Bender M., Sowers T. & Labeyrie L. (1994) The dole effect and its variations during the last 130,000 years as measured in the Vostok ice core. *Global Biogeochemical Cycles* **8,** 363–376.

Braud I., Bariac T., Gaudet J.P. & Vauclin M. (2005) SiSPAT-isotope, a coupled heat, water and stable isotope (HDO and $H_2{}^{18}O$) transport model for bare soil. Part I. Model description and first verifications. *Journal of Hydrology* **309,** 277–300.

Cappa C.D., Drisdell W.S., Smith J.D., Saykally R.J. & Cohen R.C. (2005) Isotope fractionation of water during evaporation without condensation. *Journal of Physical Chemistry B* **109,** 24391–24400.

Cernusak L.A., Arthur D.J., Pate J.S. & Farquhar G.D. (2003) Water relations link carbon and oxygen isotope discrimination to phloem sap sugar concentration in *Eucalyptus globulus*. *Plant Physiology* **131,** 1544–1554.

Cernusak L.A., Farquhar G.D. & Pate J.S. (2005) Environmental and physiological controls over oxygen and carbon isotope composition of Tasmanian blue gum, *Eucalyptus globulus*. *Tree Physiology* **25,** 129–146.

Cernusak L.A., Farquhar G.D., Wong S.C. & Stuart-Williams H. (2004) Measurement and interpretation of the oxygen isotope composition of carbon dioxide respired by leaves in the dark. *Plant Physiology* **136,** 3350–3363.

Cernusak L.A., Pate J.S. & Farquhar G.D. (2002) Diurnal variation in the stable isotope composition of water and dry matter in fruiting *Lupinus angustifolius* under field conditions. *Plant, Cell & Environment* **25,** 893–907.

Craig H. & Gordon L.I. (1965) Deuterium and oxygen-18 variations in the ocean and the marine atmosphere. Paper presented at the Stable Isotopes in Oceanographic Studies and Paleotemperatures, Spoleto, Italy.

Cuntz M., Ciais P., Hoffmann G. & Knorr W. (2003) A comprehensive global three-dimensional model of $\delta^{18}O$ in atmospheric CO_2: 1. Validation of surface processes. *Journal of Geophysical Research-Atmospheres* **108,** 4527.

Dongmann G., Nürnberg H.W., Förstel H. & Wagener K. (1974) Enrichment of $H_2{}^{18}O$ in leaves of transpiring plants. *Radiation and Environmental Biophysics* **11,** 41–52.

Easteal A.J., Edge A.V.J. & Woolf L.A. (1984) Isotope effects in water. Tracer diffusion-coefficients for $H_2{}^{18}O$ in ordinary water. *Journal of Physical Chemistry* **88,** 6060–6063.

Farquhar G.D. & Cernusak L.A. (2005) On the isotopic composition of leaf water in the non-steady state. *Functional Plant Biology* **32,** 293–303.

Farquhar G.D. & Gan K.S. (2003) On the progressive enrichment of the oxygen isotopic composition of water along a leaf. *Plant, Cell & Environment* **26,** 1579–1597.

Farquhar G.D. & Lloyd J. (1993) Carbon and oxygen isotope effects in the exchange of carbon dioxide between terrestrial plants and the atmosphere. In *Stable Isotopes and Plant Carbon-Water Relations* (eds J.R. Ehleringer, A.E. Hall & G.D. Farquhar) pp. 47–70. Academic Press, New York, NY, USA.

Farquhar G.D., Lloyd J., Taylor J.A., Flanagan L.B., Syvertsen J.P., Hubick K.T., Wong S.C. & Ehleringer J.R. (1993) Vegetation effects on the isotope composition of oxygen in atmospheric CO_2. *Nature* **363,** 439–443.

Farquhar G.D., von Caemmerer S. & Berry J.A. (1980) A biochemical-model of photosynthetic CO_2 assimilation in leaves of C_3 species. *Planta* **149,** 78–90.

Flanagan L.B. (1993) Environmental and biological influences on the stable oxygen and hydrogen isotopic composition of leaf water. In *Stable Isotopes and Plant Carbon-Water Relations* (eds J.R. Ehleringer, A.E. Hall & G.D. Farquhar) pp. 71–90. Academic Press, San Diego, CA, USA.

Flanagan L.B., Bain J.F. & Ehleringer J.R. (1991) Stable oxygen and hydrogen isotope composition of leaf water in C_3 and C_4 plant-species under field conditions. *Oecologia* **88,** 394–400.

Flanagan L.B., Comstock J.P. & Ehleringer J.R. (1991) Comparison of modeled and observed environmental-influences on the stable oxygen and hydrogen isotope composition of leaf water in *Phaseolus vulgaris* L. *Plant Physiology* **96,** 588–596.

Gvirtzman H. & Gorelick S.M. (1991) Dispersion and advection in unsaturated porous-media enhanced by anion exclusion. *Nature* **352,** 793–795.

Harris K.R. (1996) On the correlation of tracer diffusion coefficients. *Journal of Chemical and Engineering Data* **41,** 891–894.

Harris K.R. & Woolf L.A. (1980) Pressure and temperature-dependence of the self-diffusion coefficient of water and oxygen-18 water. *Journal of the Chemical Society-Faraday Transactions I* **76,** 377–385.

Harwood K.G., Gillon J.S., Griffiths H. & Broadmeadow M.S.J. (1998) Diurnal variation of $\Delta^{13}CO_2$, $\Delta C^{18}O^{16}$ and evaporative site enrichment of $\delta H_2{}^{18}O$ in *Piper aduncum* under field conditions in Trinidad. *Plant, Cell & Environment* **21,** 269–283.

Helman Y., Barkan E., Eisenstadt D., Luz B. & Kaplan A. (2005) Fractionation of the three stable oxygen isotopes by oxygen-producing and oxygen-consuming reactions in photosynthetic organisms. *Plant Physiology* **138,** 2292–2298.

Hill R. (1965) The biochemists' green mansions. The photosynthetic electron–transport chain in plants. *Essays in Biochemistry* **1,** 121–151.

James S.A. & Bell D.T. (2001) Leaf morphological and anatomical characteristics of heteroblastic *Eucalyptus globulus* ssp. globulus (Myrtaceae). *Australian Journal of Botany* **49,** 259–269.

Keeling R.F. (1995) The atmospheric oxygen cycle – the oxygen isotopes of atmospheric CO_2 and O_2 and the O_2/N_2 ratio. *Reviews of Geophysics* **33,** 1253–1262.

Lai C.T., Ehleringer J.R., Bond B.J. & U K.T.P. (2006) Contributions of evaporation, isotopic non-steady state transpiration and atmospheric mixing on the $\delta^{18}O$ of water vapour in Pacific Northwest coniferous forests. *Plant, Cell & Environment* **29,** 77–94.

Leaney F.W., Osmond C.B., Allison G.B. & Ziegler H. (1985) Hydrogen-isotope composition of leaf water in C_3 and C_4 plants – its relationship to the hydrogen-isotope composition of dry-matter. *Planta* **164,** 215–220.

Longsworth L.G. (1954) Temperature dependence of diffusion in aqueous solutions. *Journal of Physical Chemistry* **58,** 770–773.

Longsworth L.G. (1960) The mutual diffusion of light and heavy water. *Journal of Physical Chemistry* **64,** 1914–1917.

Melayah A., Bruckler L. & Bariac T. (1996) Modeling the transport of water stable isotopes in unsaturated sails under natural conditions. 1. Theory. *Water Resources Research* **32,** 2047–2054.

Merlivat L. (1978) Molecular diffusivities of $H_2{}^{16}O$, $HD^{16}O$ and $H_2{}^{18}O$ in gases. *Journal of Physical Chemistry* **69,** 2864–2871.

Mills R. (1973) Self-diffusion in normal and heavy-water in range 1–45 degrees. *Journal of Physical Chemistry* **77,** 685–688.

Mills R. & Harris K.R. (1976) Effect of isotopic substitution on diffusion in liquids. *Chemical Society Reviews* **5,** 215–231.

Ogée J., Cuntz M., Peylin P. & Bariac T. (2007) Non-steady-state, non-uniform transpiration rate and leaf anatomy effects on the progressive stable isotope enrichment of leaf water along monocot leaves. *Plant, Cell & Environment* **30,** 367–387.

Passioura J.B. (1971) Hydrodynamic dispersion in aggregated media. 1. Theory. *Soil Science* **111,** 339–344.

Passioura J.B. & Munns R. (2000) Rapid environmental changes that affect leaf water status induce transient surges or pauses in leaf expansion rate. *Australian Journal of Plant Physiology* **27,** 941–948.

Press W.H., Teukolsky S.A., Vetterling W.T. & Flannery B.P. (1992) *Numerical Recipes in C: the Art of Scientific Computing* 2nd edn. Cambridge University Press Cambridge, UK.

Price W.S., Ide H. & Arata Y. (1999) Self-diffusion of supercooled water to 238 K using PGSE NMR diffusion measurements. *Journal of Physical Chemistry a* **103,** 448–450.

Price W.S., Ide H., Arata Y. & Soderman O. (2000) Temperature dependence of the self-diffusion of supercooled heavy water to 244 K. *Journal of Physical Chemistry B* **104,** 5874–5876.

Proseus T.E., Ortega J.K.E. & Boyer J.S. (1999) Separating growth from elastic deformation during cell enlargement. *Plant Physiology* **119,** 775–784.

Rich J. (2004) *Integrated mass, solute, isotopic and thermal balances of a coastal wetland*. PhD thesis, Murdoch University, Perth, Western Australia.

Roden J.S. & Ehleringer J.R. (1999) Observations of hydrogen and oxygen isotopes in leaf water confirm the Craig-Gordon model under wide-ranging environmental conditions. *Plant Physiology* **120,** 1165–1173.

Seibt U., Wingate L., Berry J.A. & Lloyd J. (2006) Non-steady state effects in diurnal ^{18}O discrimination by *Picea sitchensis* branches in the field. *Plant, Cell & Environment* **29,** 928–939.

Shurbaji A.R.M. & Phillips F.M. (1995) A numerical-model for the movement of H_2O, $H_2{}^{18}O$, and ^2HHO in the unsaturated zone. *Journal of Hydrology* **171,** 125–142.

Taylor K.E. (2001) Summarizing multiple aspects of model performance in a single diagram. *Journal of Geophysical Research-Atmospheres* **106,** 7183–7192.

Wang J.H. (1954) Theory of the self-diffusion of water in protein solutions – a new method for studying the hydration and shape of protein molecules. *Journal of the American Chemical Society* **76,** 4755–4763.

Wang J.H., Robinson C.V. & Edelman I.S. (1953) Self-diffusion and structure of liquid water. 3. Measurement of the self-diffusion of liquid water with ^2H, ^3H, and ^{18}O as tracers. *Journal of the American Chemical Society* **75,** 466–470.

Wang X.F., Yakir D. & Avishai M. (1998) Non-climatic variations in the oxygen isotopic compositions of plants. *Global Change Biology* **4,** 835–849.

Weingärtner H. (1982) Self-diffusion in liquid water – a reassessment. *Zeitschrift für Physikalische Chemie-Wiesbaden* **132,** 129–149.

White J.W.C. (1989) A review of applications of D/H ratios in plants. In *Stable Isotopes in Ecological Systems* (eds P. Rundel, J.R. Ehleringer & K.A. Nagy) pp. 142–162. Springer-Verlag, New York, NY, USA.

Woolf L.A. (1975) Tracer diffusion of tritiated-water (THO) in ordinary water (H_2O) under Pressure. *Journal of the Chemical Society-Faraday Transactions I* **71,** 784–796.

Yakir D. (1997) Oxygen-18 of leaf water: a crossroad for plant-associated isotopic signals. In *Stable Isotopes: the Integration of Biological, Ecological and Geochemical Processes* (ed. H. Griffiths) pp. 147–168. Bios Scientific Publisher, Oxford, UK.

Yakir D., Deniro M.J. & Rundel P.W. (1989) Isotopic inhomogeneity of leaf water – evidence and implications for the use of isotopic signals transduced by plants. *Geochimica Et Cosmochimica Acta* **53,** 2769–2773.

Zimmermann U., Ehhalt D. & Münnich K.O. (1967) Soil-water movement and evapotranspiration: changes in the isotopic composition of the water. Paper presented at the Proceedings of the Symposium of Isotopes in Hydrology, Vienna, Austria.

Received 22 December 2006; received in revised form 10 April 2007; accepted for publication 11 April 2007

APPENDIX

Appendix A

List of symbols

a_1	Constant in temperature dependent description of diffusivity
a_2	Constant in temperature dependent description of diffusivity (K)
a_3	Constant in temperature dependent description of diffusivity (K^2)
A	Net assimilation rate (mol m^{-2} s^{-1})
C	Molar water concentration (mol m^{-3})
c_1	Constant in Dongmann-style solutions
C_i	CO_2 mixing ratio in stomata (ppm)
d	(Apparent) Leaf thickness (2 mesophyll thickness) (m)
D	Diffusivity (m^2 s^{-1})
D_r	Effective diffusivity in r-direction (m^2 s^{-1})
D_{H_2O}	H_2O self-diffusivity (m^2 s^{-1})
$D_{H_2{}^{18}O(H_2O)}$	Tracer diffusivity of $H_2{}^{18}O$ in 'normal' water (m^2 s^{-1})
$D_{HDO(H_2O)}$	Tracer diffusivity of HDO in 'normal' water (m^2 s^{-1})

$D_{HTO(H_2O)}$	Tracer diffusivity of HTO in 'normal' water ($m^2\ s^{-1}$)
dt	time step (s)
E	Transpiration rate (mol $m^{-2}\ s^{-1}$)
f_{em}	Factor relating bulk mesophyll water with leaf water enrichment at the evaporating site in the steady-state Péclet model
$f_{m,down}$	fraction of abaxial to apparent total mesophyll thickness
$f_{m,up}$	fraction of adaxial to apparent total mesophyll thickness
g_b	Boundary-layer conductance (mol $m^{-2}\ s^{-1}$)
g_s	Stomatal conductance (mol $m^{-2}\ s^{-1}$)
$g_{s,night}$	Night-time stomatal conductance (mol $m^{-2}\ s^{-1}$)
g_t	Total conductance (mol $m^{-2}\ s^{-1}$)
h	Relative humidity corrected to leaf temperature
J_r	Flux of tracer in mesophyll (mol $m^{-2}\ s^{-1}$)
J_x	Flux from xylem to mesophyll (mol $m^{-2}\ s^{-1}$)
k	Factor for water velocity in Farquhar & Lloyd's (1993) Péclet description
L_{eff}	Effective length of water isotopologue flow in mesophyll (m)
m_0	Mass of one mole H_2O (kg)
m_i	Mass of one mole H_2O, HDO or HTO (kg)
$\wp$	Péclet number
$\wp_l$	Longitudinal Péclet number in xylem
$\wp_m$	Péclet number in mesophyll
$\wp_{m,down}$	Péclet number in abaxial mesophyll
$\wp_{m,up}$	Péclet number in adaxial mesophyll
r	Radial coordinate (m)
r_e	Distance from xylem to evaporative site (m)
$\Re$	Correlation coefficient
$\Re^2$	Coefficient of determination
R	Isotope ratio
R_C	Craig and Gordon steady-state isotope ratio at evaporative site
R_e	Isotope ratio at evaporative site
R_E	Isotope ratio of transpiration
R_e^{ss}	Steady-state isotope ratio at evaporative site
r_m	Mesophyll thickness (m)
$r_{m,down}$	Abaxial mesophyll thickness (m)
$r_{m,up}$	Adaxial mesophyll thickness (m)
R_m	Isotope ratio of bulk mesophyll
R_s	Isotope ratio of plant available source water
R_v	Isotope ratio of ambient water vapour
r_x	Radial coordinate at xylem-mesophyll interface (m)
R_x	Isotope ratio of xylem to mesophyll flux
t	time dimension (s)
v	Advection velocity (m s^{-1})
v_e	Advection velocity at the evaporative sites (m s^{-1})
V_m	Mesophyll water volume (mol m^{-2})
$V_{m,const}$	Mean observed mesophyll water volume (mol m^{-2})
$V_{m,const\text{-}max}$	Maximum observed mesophyll water volume (mol m^{-2})
$V_{m,const\text{-}min}$	Minimum observed mesophyll water volume (mol m^{-2})
$V_{m,down}$	Water volume of abaxial mesophyll (mol m^{-2})
$V_{m,up}$	Water volume of adaxial mesophyll (mol m^{-2})
v_r	Effective advection velocity in r-direction (m s^{-1})
w_a	Ambient humidity in mol(H_2O) mol(air)$^{-1}$
w_i	Humidity in the stomatal cavity mol(H_2O) mol(air)$^{-1}$
α^+	Equilibrium water-vapour fractionation factor
α_k	Kinetic fractionation factor
Δ	Isotope ratio relative to source water
Δ_C	Craig and Gordon steady-state isotope ratio at evaporative site relative to source water
Δ_e	Isotope ratio at evaporative site relative to source water
Δ_E	Isotope ratio of transpiration relative to source water
Δ_m	Isotope ratio of bulk mesophyll relative to source water
$\Delta_{m,down}$	Isotope ratio of abaxial bulk mesophyll relative to source water
$\Delta_{m,up}$	Isotope ratio of adaxial bulk mesophyll relative to source water
Δ^2H_m	Hydrogen isotope ratio of bulk mesophyll relative to source water
$\Delta^{18}O_m$	Oxygen isotope ratio of bulk mesophyll relative to source water
Δ_m^{ss}	Steady-state isotope ratio of bulk mesophyll relative to source water
Δ_x^{ss}	Steady-state isotope ratio of bulk xylem relative to source water
Θ_m	Volumetric liquid water content
$\Theta_{m,down}$	Volumetric liquid water content of abaxial mesophyll
$\Theta_{m,up}$	Volumetric liquid water content of adaxial mesophyll
$\kappa_{apoplastic}$	Tortuosity factor of apoplastic water pathway
κ_m	Tortuosity factor of in mesophyll
$\kappa_{m,down}$	Tortuosity factor of in abaxial mesophyll
$\kappa_{m,up}$	Tortuosity factor of in adaxial mesophyll
$\kappa_{symplastic}$	Tortuosity factor of symplastic water pathway
$\kappa_{transcellular}$	Tortuosity factor of transcellular water pathway
$\hat{\sigma}$	Normalized SD
μ_i	reduced mass of water isotopologue in 'normal' water (kg)
χ	Tracer concentration (mol m^{-3})

Appendix B

Craig and Gordon model

Considering the stomatal opening as a resistance to diffusion of water vapour, the transpiration rate E (mol m^{-2} s^{-1}) can be written as (for symbol definition, see the list of symbols in Appendix A):

$$E = g_t(w_i - w_a). \tag{A1}$$

The same flux scheme can be written for the heavier isotopologue $E' = R_E E$ (with $R_E << 1$, that is, $E \cong E_{H_2^{16}O}$):

$$R_E E = \frac{g_t}{\alpha_k}\left(\frac{R_e}{\alpha^+} w_i - R_v w_a\right) \tag{A2}$$

with $\alpha^+ > 1$ and $\alpha_k > 1$. This leads to the Craig and Gordon model without the steady-state assumption:

$$R_E = \frac{1}{\alpha^+\alpha_k(1-h)}(R_e - \alpha^+ h R_v). \tag{A3}$$

In the steady state, it is apparent that transpiration must have the same isotopic composition as the supplying water, that is, $R_E = R_s$, so that this becomes the so-called Craig and Gordon steady-state model:

$$R_e^{ss} = R_C = \alpha^+\alpha_k(1-h)R_s + \alpha^+ h R_v. \tag{A4}$$

Farquhar & Cernusak (2005) non-steady-state model

Writing the mass balance equations for the different water isotopologues in the mesophyll gives for $H_2^{16}O$:

$$\frac{dV_m}{dt} = J_x - E. \tag{A5}$$

This means that mesophyll water volume V_m (mol m^{-2}) will be diminished by transpiration E, but it will be refilled by a flux from the leaf veins (or xylem) J_x. Writing the analogous mass balance for $H_2^{18}O$ (or HDO) gives

$$\frac{d(R_m V_m)}{dt} = R_x J_x - R_E E. \tag{A6}$$

There is a continuity of the flux at the xylem–mesophyll interface (Farquhar & Gan 2003), that is, the incoming flux is $R_s J_x$. With this boundary condition and the H_2O mass balance (Eqn A5), this becomes

$$\frac{d(R_m V_m)}{dt} = R_s \frac{dV_m}{dt} - (R_E - R_s)E, \tag{A7}$$

or in Δ notation,

$$\frac{d(\Delta_m V_m)}{dt} = -\Delta_E E. \tag{A8}$$

The isotopic composition of transpiration Δ_E is directly linked to the isotopic composition at the evaporating sites by the Craig and Gordon equation without the steady-state assumption (Eqn A3), and also substituting in the Craig and Gordon steady-state equation (Eqn A4), this can be written as

$$\frac{d(\Delta_m V_m)}{dt} = \frac{g_t w_i}{\alpha^+\alpha_k}(\Delta_C - \Delta_e), \tag{A9}$$

where $g_t w_i$ can be seen as the one-way flux from the stoma into the atmosphere. This formulation links the change in isotopic bulk mesophyll water Δ_m to the isotopic composition at the evaporating site Δ_e. To solve this (Eqn A9), one needs to know how both quantities are linked together in time. The idea of Farquhar & Cernusak (2005) was to assume that in non-steady state, there is still an exponential isotope profile in the mesophyll from the xylem to the evaporating sites, and that this profile has the same form as in steady state:

$$\Delta_m = f_{em}\Delta_e \tag{A10}$$

$$f_{em} = \frac{1 - e^{-\wp_m}}{\wp_m}. \tag{A11}$$

This assumption links the isotopic composition at the evaporating sites Δ_e with the bulk isotopic composition Δ_m, so that the Farquhar & Cernusak (2005) non-steady-state model can be written as an ordinary differential equation (ODE):

$$\frac{d(\Delta_m V_m)}{dt} = \frac{g_t w_i}{\alpha^+\alpha_k}\left(\Delta_C - \frac{\Delta_m}{f_{em}}\right). \tag{A12}$$

Solution to the Farquhar & Cernusak (2005) and earlier non-steady-state models

Farquhar & Cernusak (2005) give a closed analytical solution for their ODE (Eqn A12) if one knows the time course of V_m, E, h and Δ_C. But even linear evolutions of these variables lead to integrals that are almost impossible to solve. Another possibility for solving this equation is to assume that at time t, the environmental conditions change to a new value and stay constant for a certain time dt, that is, making a step change in the environmental conditions (Dongmann *et al.* 1974). This is strictly incorrect because, for example, either mesophyll water volume V_m is constant and then dV_m/dt must be zero or dV_m/dt is not zero and then V_m cannot be constant. However, the smaller the time step dt, the smaller the error in this form of solution. The general iterative solution of Eqn A12 is

$$\Delta_m(t+dt) = c_1\Delta_C + [\Delta_m(t) - c_1\Delta_C] \exp\left\{-\frac{g_t w_i}{\alpha^+\alpha_k V_m c_1} dt\right\}. \tag{A13}$$

We call this type of iterative solution the 'Dongmann-style solution'. It turns out that to our knowledge, all earlier

formulations of one-dimensional non-steady-state leaf water enrichment can be solved in this iterative form with different constant c_1:

1 Dongmann *et al.* (1974) and later Bariac *et al.* (1994) assume constant water volume V_m and make no distinction between bulk mesophyll water Δ_m and leaf water at the evaporating site Δ_e, that is, $c_1 = 1$.
2 Cernusak *et al.* (2002) assume $\Delta_m = \Delta_e$ but varying water volume V_m, that is, $\frac{1}{c_1} = 1 + \frac{\alpha_k \alpha^+}{g_t w_i}\frac{dV_m}{dt}$.
3 In the case of Farquhar & Cernusak (2005), V_m is varying and $\Delta_m = f_{em}\Delta_e$, that is, $\frac{1}{c_1} = \frac{1}{f_{em}} + \frac{\alpha_k \alpha^+}{g_t w_i}\frac{dV_m}{dt}$.
4 For completeness, one can construct the case when V_m is constant and $\Delta_m = f_{em}\Delta_e$, that is, $c_1 = f_{em}$.

Relating advection–diffusion to Farquhar & Lloyd's (1993) steady-state Péclet effect

The Péclet effect as written by Farquhar & Lloyd (1993) is only valid in the steady state, that is, the isotopic composition of water leaving the leaf by transpiration is equal to that entering the mesophyll from the xylem, and the bulk mesophyll water isotopic composition is constant. The term $\partial R/\partial t$ in the advection–diffusion equation (Eqn 9) is then zero. The original equation of Farquhar & Lloyd (1993) assumed also no change in leaf water content. If leaf water content does not change, there is no velocity profile and v_r is constant. The solution of Eqn 9 with $\partial R/\partial t = 0$, and the boundary conditions Eqns 12 and 13 with $v_r = E/2C$ is

$$R(r) = R_s + [R_C - R_s]\exp\left\{-\frac{\wp_m}{r_m}(r_e - r)\right\}, \tag{A14}$$

with $\wp_m = Er_m/2CD_r$. This means that the isotope ratio in steady state diminishes from R_C at the evaporating site ($r = r_e$) to $R_s + (R_C - R_s)e^{-\wp_m}$, and not R_s, at the xylem–mesophyll interface ($r = r_x$). Written in Δ notation this is

$$\Delta(r) = \Delta_C \exp\left\{-\frac{\wp_m}{r_m}(r_e - r)\right\}. \tag{A15}$$

The mean Δ between r_x and r_e is then just the Péclet formulation of Farquhar & Lloyd (1993):

$$\Delta_m^{ss} = \Delta_C \frac{1 - e^{-\wp_m}}{\wp_m}. \tag{A16}$$

Relating advection–diffusion to the Farquhar & Cernusak (2005) non-steady-state model

To relate the present advection–diffusion description to the formulation of Farquhar & Cernusak (2005), we integrate Eqn 9 from r_x to r_e, divide by r_m (averaging) and use the relation between $\partial v_r/\partial r$ and $\partial\Theta_m/\partial t$ (Eqn 7):

$$\begin{aligned}\frac{\partial R_m}{\partial t} &= \frac{1}{r_m\Theta_m}\left[-v_r R|_{r_x}^{r_e} + \int_{r_x}^{r_e} R\frac{\partial v_r}{\partial r'}dr' + D_r\frac{\partial R}{\partial r}\Big|_{r_x}^{r_e}\right] \\ &= \frac{1}{r_m\Theta_m}\Big[-v_r(r_e,t)R(r_e,t) + v_r(r_x,t)R(r_x,t) - \\ &\quad r_m R_m\frac{\partial\Theta_m}{\partial t} + D_r\frac{\partial R}{\partial r}\Big|_{r_e,t} - D_r\frac{\partial R}{\partial r}\Big|_{r_x,t}\Big],\end{aligned} \tag{A17}$$

where we integrated by parts the first term of the right-hand side of Eqn 9. Using the boundary conditions (Eqns 12 and 13) gives

$$\Theta_m\frac{\partial R_m}{\partial t} + R_m\frac{\partial\Theta_m}{\partial t} = \frac{1}{r_m}[-v_r(r_e,t)R_E + v_r(r_x,t)R_s]. \tag{A18}$$

Using the linear velocity profile (Eqn 10) and switching to Δ notation leads almost to Eqns A8 (and A9):

$$\frac{d(\Delta_m\Theta_m C r_m)}{dt} = -\Delta_E E/2. \tag{A19}$$

The xylem is situated rather in the middle of the leaf. The advection–diffusion equation calculates from the xylem ($r = r_x$) to the evaporating side ($r = r_e$), that is, it calculates only one side of the mesophyll. $\Theta_m C r_m$ is therefore the water volume of half the mesophyll. If both halves of the leaf (adaxial and abaxial) are the same, each is $V_m/2$, and this yields exactly Eqns A8 (and A9).

The advection–diffusion equation (Eqn 9) does not lead to the ODE of Farquhar & Cernusak (2005) (Eqn A12) because this includes the assumption about the shape of the isotope profile. The advection–diffusion equation makes no assumption about the isotope profile from the xylem to the mesophyll but rather calculates exactly this profile.

Leaf parameters for the adaxial and abaxial leaf sides

Mesophyll water volume V_m is linked to volumetric mesophyll water content Θ_m (for symbol definition, see the list of symbols in Appendix A):

$$\begin{aligned}V_{m,up} &= \Theta_{m,up}Cr_{m,up} = \Theta_{m,up}Cf_{m,up}d \\ V_{m,down} &= \Theta_{m,down}Cr_{m,down} = \Theta_{m,down}Cf_{m,down}d \\ V_m &= (\Theta_{m,up}f_{m,up} + \Theta_{m,down}f_{m,down})Cd = \Theta_m Cd \\ \Theta_m &= \Theta_{m,up}f_{m,up} + \Theta_{m,down}f_{m,down}\end{aligned} \tag{A20}$$

with $r_{m,up} = f_{m,up}d$, $r_{m,down} = f_{m,down}d$ and $f_{m,up} + f_{m,down} = 1$. The tortuosity factor κ_m is taken to be the same in the adaxial and abaxial mesophyll so that it relates to half the leaf thickness d:

$$\kappa_{m,up} = \kappa_{m,down} = \kappa_m = \frac{d/2}{\Theta_m L_{eff}}. \tag{A21}$$

In order to calculate one advection–diffusion equation for each mesophyll side separately, one needs to know or estimate the relative thickness of both mesophylls, $f_{m,up} = r_{m,up}/d$ and $f_{m,down} = r_{m,down}/d$, and the volumetric water

contents $\Theta_{m,up}$ and $\Theta_{m,down}$. The water variables and (apparent) leaf thickness follow then from Eqn A20 with the measured mesophyll water volume V_m. One needs to estimate an effective length L_{eff} or tortuosity factor κ_m. Because L_{eff} is a tuning parameter for the amplitude of the model, this is carried out with Θ_m at midday. The advection–diffusion model uses a fixed tortuosity factor κ_m and a fixed length r_m instead of an effective length L_{eff}. The apparent L_{eff} in the Péclet number $\wp$ depends then on the varying Θ_m and is therefore not constant.

We estimated the leaf parameters for *Lupinus angustifolius* from cross-sections of typical dicotyledonous leaves (e.g. Atwell *et al.* 1999) to $f_{m,up} = 0.6$, $f_{m,down} = 0.4$, $\Theta_{m,up} = 0.9$ and $\Theta_{m,down} = 0.5$. We took the values of James & Bell (2001) for *Eucalyptus globulus*: $f_{m,up} = 0.6$, $f_{m,down} = 0.4$, $\Theta_{m,up} = 0.9$ and $\Theta_{m,down} = 0.7$. The estimated effective lengths L_{eff} are explained in the main text.

Our extreme estimates for the lupin simulations of Fig. 3b are $f_{m,up} = 0.7$, $f_{m,down} = 0.3$, $\Theta_{m,up} = 1.0$ and $\Theta_{m,down} = 0.3$.

Diffusivity D

In the literature of leaf water enrichment, the diffusivity D is normally taken as constant: $2.66 \cdot 10^{-9}$ m^2 s^{-1} for $H_2{}^{18}O$ and $2.34 \cdot 10^{-9}$ m^2 s^{-1} for HDO, respectively. The values are supposed to come from a paper of Wang (1954), but this was a mistaken citation, which was carried forward through subsequent publications. The values come from Wang, Robinson & Edelman (1953) and were measured at 25 °C. However, diffusivity D is not constant but is temperature dependent. Additionally, the turbulent stirring method of Wang *et al.* (1953) 'tends to give values that are too high' (Weingärtner 1982).

Measurements of H_2O self-diffusivity (D_{H_2O}) and tracer diffusivity of tritiated water in 'normal' water [$D_{HTO(H_2O)}$] were performed by Mills (1973) at different temperatures. He also reports measurements of tracer diffusivity of deuterated water in 'normal' water ($D_{HDO(H_2O)}$) of Longsworth (1954, 1960). Easteal, Edge & Woolf (1984) reported values for the diffusivity of $H_2{}^{18}O$ in 'normal' water [$D_{H_2{}^{18}O(H_2O)}$] between 0 and 50 °C with an accuracy of about 0.3%. The exact form of the temperature dependence of tracer and self-diffusivity is unknown, but two functional forms that work well are firstly a derivative of an Arrhenius plot (Mills 1973; Woolf 1975):

$$D = 10^{-9} \exp\{a_1 + a_2/T + a_3/T^2\}, \qquad \text{(A22)}$$

and secondly, a Vogel–Tamman–Fulcher relationship (VTF) (Price, Ide & Arata 1999; Price *et al.* 2000):

$$D = a_1 \cdot 10^{-9} \exp\left\{-\frac{a_2}{T - a_3}\right\}, \qquad \text{(A23)}$$

where a_1, a_2 and a_3 are constant parameters. We show in Fig. A1b,c the measurements and fitted curves of the tracer diffusivities of water isotopologues in 'normal' water. Both functional forms perform equally well and are indistinguishable on the plot (so only the VTF is shown as the solid line). Table A1 records the parameters a_1–a_3 for both functional forms including their uncertainties. The values of the Arrhenius type relationship can be compared to the values obtained by Easteal *et al.* (1984).

Table A1. Fitted parameters to the Arrhenius derived and the Vogel–Tamman–Fulcher (VTF) relationship of tracer and self-diffusivity of water

	Arrhenius			VTF		
	a_1	a_2	a_3	a_1	a_2	a_3
H_2O	–1.2	2055	–634783	100	577	145
	(0.2)	(137)	(20167)	(6)	(18)	(2)
$H_2{}^{18}O$	–0.4	1528	–554368	119	637	137
	(1.6)	(959)	(143446)	(55)	(151)	(19)
HDO	–0.7	1729	–586977	116	626	139
	(1.4)	(807)	(118620)	(45)	(121)	(15)
HTO	–1.3	2082	–638900	097	574	146
	(0.2)	(142)	(21006)	(6)	(19)	(2)

Number in parentheses give the uncertainties of the parameters. H_2O stands for H_2O self-diffusivity, and $H_2{}^{18}O$, HDO and HTO stand for tracer diffusivities in 'normal' water.

Tracer diffusivities of HDO and HTO, and H_2O self-diffusivity seem to be proportional to each other with the square root of the reduced masses, at least under atmospheric pressure (Mills & Harris 1976; Harris & Woolf 1980; Harris 1996):

$$\frac{D_i}{D_j} = \left(\frac{\mu_j}{\mu_i}\right)^{\frac{1}{2}} \quad \text{with} \quad \mu_i = \frac{m_i m_0}{m_i + m_0} \; i \in (0, 1, 2), \qquad \text{(A24)}$$

the index i denoting $0 \equiv H_2O$, $1/2 \equiv$ HDO/HTO. This means that the constants a_2 and a_3 should be the same in Fig. A1c,d, which they are only approximately. The data of Harris & Woolf (1980) suggest that there is 'a slightly greater coupling of translational and rotational motion of HTO relative to H_2O in pure water at low pressures'. However, the pressure dependency effect of Harris & Woolf (1980) is rather small and most likely negligible at atmospheric pressures.

For $H_2{}^{18}O$, tracer diffusivity slightly deviates from the pure mass relationship with other diffusivities (Easteal *et al.* 1984). But this effect is small at atmospheric pressure. However, the mean ratio of $D_{H_2{}^{18}O(H_2O)}$ and D_{H_2O} does not follow Eqn A24: $D_{H_2O}/D_{H_2{}^{18}O(H_2O)} \approx 1.011$ instead of 1.026 (Eqn A24).

However, all measurements of water isotopologue tracer diffusivity were carried out in pure water. It is likely that the tracer diffusivities have lower values in solutions (such as in plant cells), whereas the temperature dependence should be very similar (Harris, personal communication).

We therefore fitted one single function to all tracer and self-diffusivities, where the tracer diffusivities were multiplied by the ratio of the reduced masses to put them

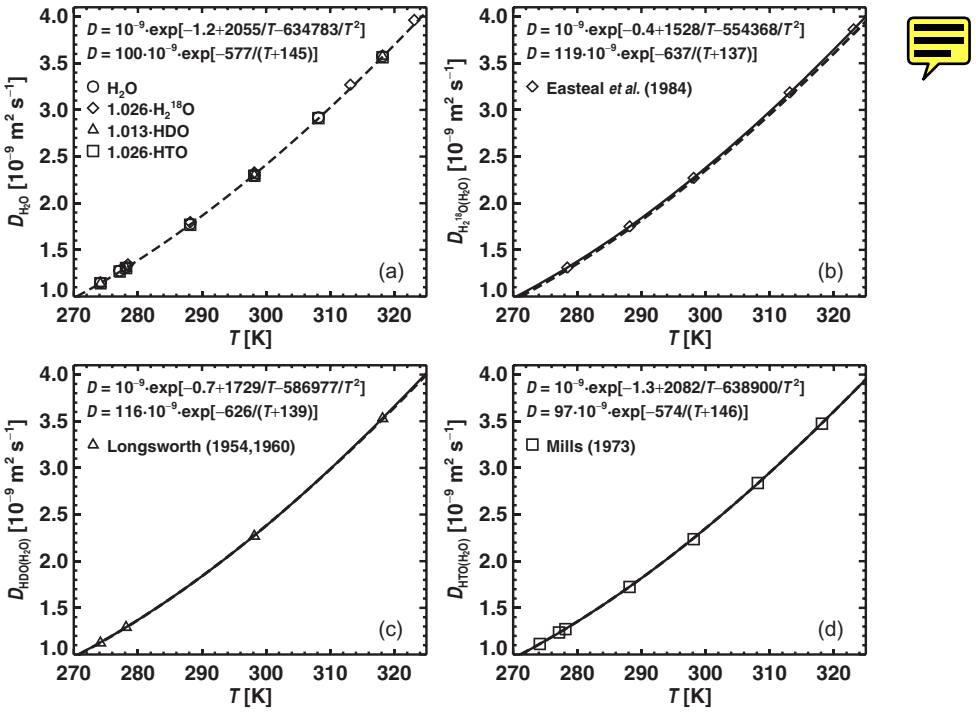

Figure A1. Temperature dependence of tracer and self-diffusivity of water: (a) combined H_2O self-diffusivity D_{H_2O}, (b) $H_2{}^{18}O$ tracer diffusivity $D_{H_2{}^{18}O(H_2O)}$, (c) HDO tracer diffusivity $D_{HDO(H_2O)}$ and (d) HTO tracer diffusivity in 'normal' water $D_{HTO(H_2O)}$. Diamonds are measurements of Easteal *et al.* (1984); triangles are measurements of Longsworth (1954, 1960) as cited by Mills (1973), and squares (HTO) and circles (H_2O) are measurements of Mills (1973). Measurement precision is, in all cases, smaller than the symbol dimensions. Solid lines are Vogel–Tamman–Fulcher (VTF) relationships to the individual tracer diffusivities, and dashed lines are the VTF relationship for all data where the tracer diffusivities are multiplied by the ratio of the reduced masses. The figure illustrates the non-linear nature of tracer and self-diffusivity of water across a biologically relevant range of temperatures.

on the same scale as the H_2O self-diffusivity (Fig. A1a & Table A1). This means that the measurements of $D_{HDO(H_2O)}$ were multiplied by $[19/18\cdot(18+18)/(18+19)]^{0.5} \approx 1.013$, and the measurements of $D_{H_2{}^{18}O(H_2O)}$ and $D_{HTO(H_2O)}$ were multiplied by $[20/18\cdot(18+18)/(18+20)]^{0.5} \approx 1.026$. Note that we included only the measurements of H_2O self-diffusivity of Mills (1973) and not of Price *et al.* (1999) because of the uncertainty of temperature measurements in magnetic resonance systems. This gives an excellent fit where the small uncertainties in the parameters a_1–a_3 stem mostly from the small uncertainties in $D_{HTO(H_2O)}$. We included in Fig. A1c,d the overall VTF fits with $a_2 = 577$, $a_3 = 145$ and $a_1 = 100/1.026$, $100/1.013$ and $100/1.026$ for $H_2{}^{18}O$, HDO and HTO, respectively (dashed lines). The values of the Arrhenius type relationship can be compared to Braud *et al.* (2005).

We think that this level of detail is sufficient in the context of leaf water isotope enrichment, because firstly, only the effective diffusivity D_r is important, and this includes the unknown tortuosity factor κ_m; secondly, because the measured diffusivities were carried out in pure water and are likely to be lower in leaf water; and thirdly, because diffusivities are much more sensitive to temperature than to an eventual bias. So in this study, we take the VTF relationship fitted to all tracer and self-diffusivities with the values of a_1–a_3 given in the previous paragraph.

